We are IntechOpen, the world's leading publisher of Open Access books Built by scientists, for scientists

4,800
Open access books available

122,000
International authors and editors

135M
Downloads

Our authors are among the

154
Countries delivered to

TOP 1%
most cited scientists

12.2%
Contributors from top 500 universities

CLARIVATE ANALYTICS BOOK CITATION INDEX INDEXED

WEB OF SCIENCE™

Selection of our books indexed in the Book Citation Index in Web of Science™ Core Collection (BKCI)

Interested in publishing with us?
Contact book.department@intechopen.com

Numbers displayed above are based on latest data collected.
For more information visit www.intechopen.com

8

The Photodiode Array: A Critical Cornerstone in Cardiac Optical Mapping

Herman D. Himel IV[1], Joseph Savarese[2] and Nabil El-Sherif[2,3]
[1]*Duke University, Durham, NC*
[2]*VA New York Harbor Healthcare System, Brooklyn, NY*
[3]*Downstate Medical Center, State University of New York, Brooklyn, NY*
USA

1. Introduction

The human heart pumps oxygenated blood to the organs and extremities in order to maintain normal physiologic function, while simultaneously pumping deoxygenated blood to the lungs for reoxygenation. Coordinated contraction of individual cardiac myocytes provides the mechanical force necessary to produce sufficient pressure and ensure that distant organs and extremities remain oxygenated. Before cardiac myocytes may contract, they must undergo excitation in order to begin the sequence of events which results in an intracellular calcium (Ca_i) rise, which in turn precipitates actin-myosin binding and ultimately results in contraction. The electrical signature of this series of events is reflected in the cardiac action potential (AP), a segment of a transmembrane voltage (V_m) recording which indicates electrical excitation (depolarization) and relaxation (repolarization) of the myocardium.

The duration, amplitude, upstroke velocity (dV_m/dt), and overall morphology of the cardiac AP are important markers of the electrical status of the heart. Studies of the cardiac AP have provided important insights into the mechanisms which drive the transition from a normal, healthy heartbeat toward a deadly cardiac arrhythmia.

Early recordings of the cardiac AP were obtained using microelectrodes (Coraboeuf & Weidmann, 1949a; Coraboeuf & Weidmann, 1949b; Draper & Weidmann, 1951; Sano et al., 1959; Sano et al., 1960; Weidmann, 1951). Although this method was highly effective in tracking temporal changes in the V_m of individual cells, the method could not be easily applied to the problem of tracking excitation over a region of tissue. Extracellular electrode mapping offered a partial solution to this problem and was sufficient to determine activation times in regions of tissue, but with this method the details of repolarization were lost and had to be estimated using indirect indicators. Further, this method required that the electrodes be in direct contact with the tissue. This made defibrillation studies difficult, since large amplitude defibrillation shocks typically obscure the details of activation during electrical recordings. Monophasic action potential (MAP) recordings were capable of elucidating the details of repolarization without damaging tissue, and have even been recorded in the beating human heart using a cardiac catheter (Shabetai et al., 1968). However they too were restricted by having little or no spatial resolution and could not be

placed in close contact with each other. As with extracellular electrodes, MAP recordings also require that the electrodes be placed in contact with the tissue.

With the emergence of V_m-sensitive dyes in the 70's, it became possible to interrogate cardiac tissue optically (Salama, 1976), and soon afterward optical methods were developed to interrogate multiple spots simultaneously in a small (~cm^2) region of tissue. Since then the field of cardiac optical mapping (COM) has greatly expanded in scope, from relatively simple early recordings using one or relatively few spots (Morad & Dillon, 1981; Salama, 1976) to highly complex optical systems. These include high spatiotemporal resolutions systems (Choi et al., 2007), panoramic systems (Kay et al., 2004; Rogers et al., 2007), and systems which are capable of interrogating electrophysiological activity beneath the surface (Byars et al., 2003). In addition, several labs have used photodiode-based optical mapping systems to map V_m and Ca_i simultaneously, on both the whole heart (Choi & Salama, 2000; Lakireddy et al., 2006; Laurita & Singal, 2001; Pruvot et al., 2004) and in monolayer cell cultures of cardiac myocytes (Fast, 2005; Fast & Ideker, 2000; Lan et al., 2007).

Cardiac optical mapping systems have greatly increased our understanding in nearly all areas of cardiac electrophysiology, from basic studies of conduction patterns (Cabo et al., 1994; Knisley & Hill, 1995) and effects of fiber geometry (Knisley & Baynham, 1997; Knisley et al., 1994; Knisley et al., 1999; Neunlist & Tung, 1995) to more clinical studies of defibrillation (Al-Khadra et al., 2000; Fast et al., 2002; Federov et al., 2008; Tung & Cysk, 2007) and ablation therapy (Himel et al., 2007; Perez et al., 2006). Although COM has not yet led to a widely accepted method of three-dimensional cardiac tissue interrogation, there have been significant advances in this area as well. Investigators have successfully used optical surface recordings to determine wavefront orientation beneath the surface (Hyatt et al., 2005; Zemlin et al., 2008), and also to interrogate deeper layers of tissue using transillumination methods (Baxter et al., 2001) and deeper-penetrating, near-infrared fluorescing dyes (Matiukas et al., 2006; Matiukas et al., 2007; Salama et al., 2005).

Photodiode sensors were used in some of the earliest optical recordings of cardiac APs (Morad & Salama, 1979; Salama, 1976), and continue to be used today (Cheng, 2006; Sakai, 2008). Photodiodes function by transferring incoming photonic energy to bound electrons in a semi-conductive material in a transistor configuration. These energized electrons may then cross from one side of the transistor to the other, resulting in a voltage difference between the two sides.

If a wire is connected from one side of the photodiode to the other while the photodiode is receiving photonic energy, current will flow in a linear fashion with respect to the input intensity of the collected light (Scherz, 2007). This makes photodiodes an excellent choice as a detector in COM systems, and this fact has been reflected by their widespread use over the past 30 years. Examples of optical APs and activation maps recorded with a photodiode array-based system are shown in figure 1.

Although other technologies such as CMOS and CCD cameras have recently gained popularity due to their higher spatial resolution, photodiode systems remain in use due to their ruggedness, high signal-to-noise ratios, excellent temporal resolution, versatility, and low cost. Recently, for example, photodiodes and photodiode arrays (PDAs) have been used in the construction of optrodes, a novel technique used to record optical signals from deeper intramural regions within the ventricular wall (Byars et al., 2003; Caldwell et al., 2005; Hooks et al., 2001; Kong et al., 2007).

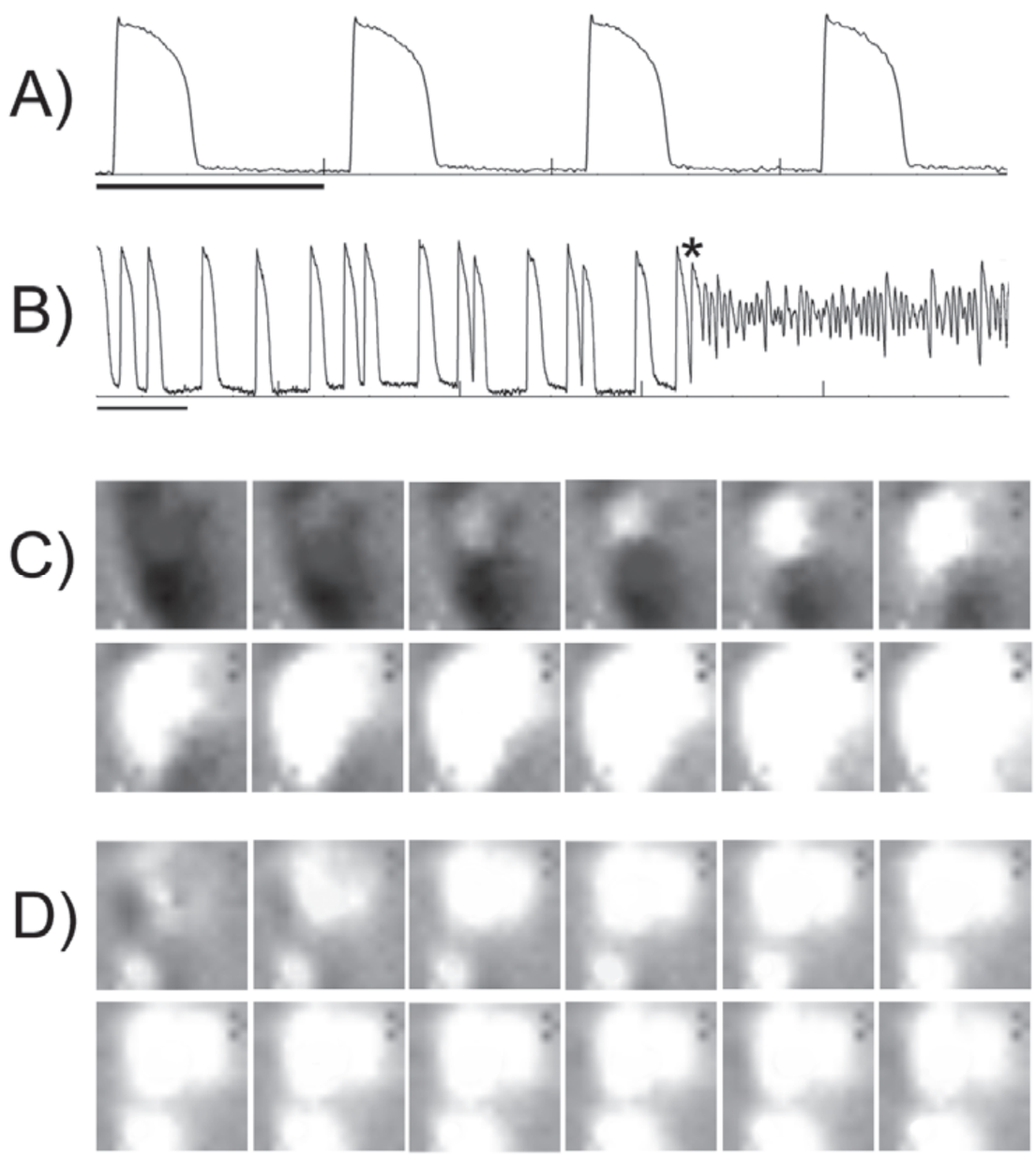

Fig. 1. APs and activation maps for normal and irregular rhythms. For rows A and B, the horizontal bar beneath each recording indicates 1 second. Row A shows APs recorded during basic rhythm. Row B shows APs occurring with irregular diastolic intervals, followed by a long run of a ventricular tachyarrhthmia, triggered by the AP marked with an asterisk. The two rows in section C show a sequence of activation during basic rhythm, while the two rows in section D show a sequence of activation which took place during a premature beat which precipitated a sustained ventricular tachyarrhythmia (note the presence of two distinct activation sites). Frames are read from left to right, and then top to bottom. Each successive frame is 1 ms apart. Lighter areas on the map indicate tissue undergoing activation.

2. Basic principles of cardiac optical mapping

Epi-illumination occurs when the fluorescence emission detector is placed on the same side of the tissue as the excitation source, whereas with trans-illumination the detector and excitation source are placed on opposite sides. For monolayer mapping systems, both epi and trans-illumination are possible since cardiac monolayers are typically only a few tens of micrometers thick. For whole-heart mapping systems which map excitation on the surface of the intact heart preparations, epi-illumination is the preferred method since very little fluorescence is transmitted through the relatively thick myocardial wall.

The tissue being mapped must be illuminated using an excitation source, which excites at least one parameter-sensitive dye in order to elicit a fluorescent signal. Changes in a targeted physiological parameter cause changes in the properties of the dye (e.g., a conformational change in the dye molecules). This results in a change in the emission spectrum of the dye, which is then recorded by a detector (e.g., a PDA), digitized, and stored on a PC for post-experimental analysis.

Changes in fluorescence due to changes in the physiological parameter are often measured as a fraction of the baseline fluorescence. This is an important parameter in optical mapping, and is known as fractional fluorescence ($\Delta F/F$). Fractional fluorescence is useful because it is a way to measure the effectiveness of a particular dye in transducing a physiological change into recordable fluorescent signal. Fractional fluorescence also indicates the general effectiveness of the system, and higher $\Delta F/F$ values are typically accompanied by higher signal-to-noise ratios. Transmembrane voltage is the most commonly studied physiological parameter in optical mapping, but intracellular calcium transients (Ca_iT) have also been studied extensively.

There are several variations of the COM system, however there are basic components that are common to all systems. These basic components include an excitation source, detector, and electronic components used for digitization, filtration, and multiplexing. A schematic for a typical whole-heart mapping system is shown in figure 2.

2.1 Excitation source

The excitation source may be either focused (i.e. laser light) or broadfield illumination (using halogen, tungsten, or more recently, high-power LED sources). Laser and some LED light sources have sufficiently narrow bands so as not to interfere with the fluorescence emission, however broadfield sources should be pre-processed using optical filters in order to decrease the width of their wavelength spectrum before illuminating the target (e.g., the heart). In general, brighter excitation sources lead to higher $\Delta F/F$ values, however the intensity of the excitation source cannot be increased without regard for *photobleaching*, which occurs when the dye emission decreases in intensity due to overexposure to excitation light (Knisley et al., 2000; Kong et al., 2003). A highly stable source is superior to a brighter but noisier source, since the stable source yields greater S/N ratios while allowing longer duration recordings.

2.2 Detector

There are several types of detectors that are currently in use for COM, however the focus of this review is upon those detectors which are photodiode-based. Other detector types will be discussed for the purpose of comparison.

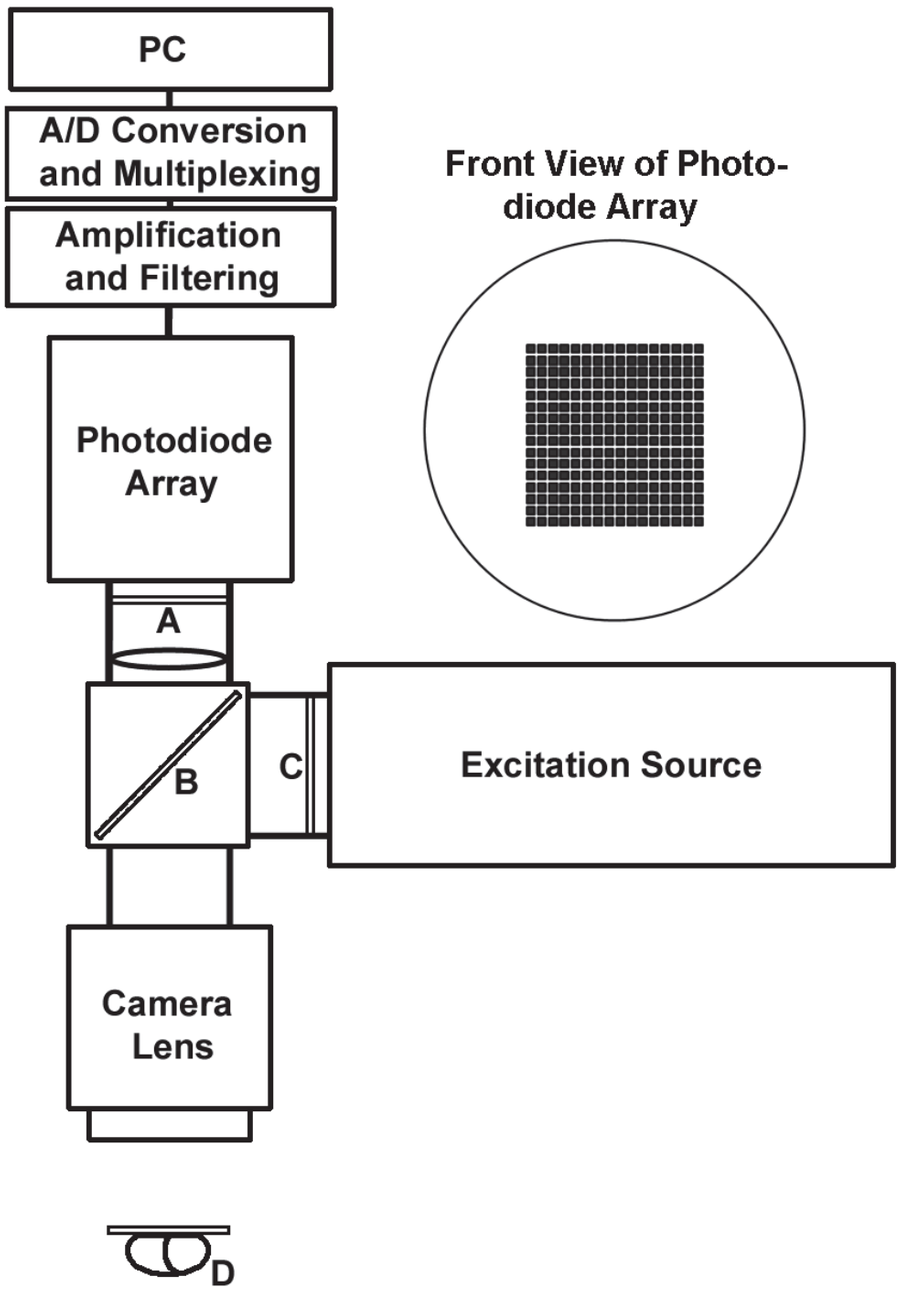

Fig. 2. Top-down view of a typical PDA-based optical mapping system. The thin rectangular boxes marked A, B, and C represent fluorescence band pass, long pass, and excitation band pass filters, respectively. The long pass filter B is housed in an optical cube. The elliptical shape between A and B represents a condensing lens. The front view of the PDA shows the 16x16 element photoactive region of the detector. The oval-like shape marked D represents the heart, which is pressed against a flat plate in order to create a two-dimensional surface so that the entire mapped region lies within the focal plane. Electrically connected components are separated by a thin solid line, while optically connected components are separated by hollow rectangles.

Current alternatives to PDAs include photomultiplier (PMT) systems, charge-coupled device (CCD) cameras, and complimentary metal-oxide semiconductor (CMOS) cameras. PMT systems have an extremely high gain (up to 10^8 increase in intensity), and can even be used in a process call "photon counting" whereby the release of individual photons may be recorded. PMT systems are capable of extremely high sensitivity, and typically have a quicker response time than photodiode systems. However for normal optical mapping applications, the sensitivity and response time of photodiodes is more than sufficient. Typically, PMT systems employ sequential rather than simultaneous recordings of adjacent spots. However, due to their rapid response time they may be coupled with a laser scanner to produce acquisition rates equivalent to those seen in photodiode-based systems. For example, a laser scanner which scans at 256 kHz with a 256-spot grid is essentially equivalent to a PDA-based 256-spot system which scans at a rate of 1 kHz. For this example, there will be a time difference of ~1 ms between the 1st and 256th spots scanned. This difference can often be neglected during normal propagation in cardiac tissue. The basis for the photomultiplier tube is the *photoelectric effect*, whereby an incident photon strikes a photocathode and starts a chain reaction. The photocathode emits an electron, which strikes subsequent dynodes, at each step of the way releasing a greater number of electrons than those which struck the preceding dynode. At the final anode, the signal has been "multiplied" many fold (~10^6) and the resultant electrons result in a change in voltage.

Cameras using CCD technology typically have impressive spatial resolution, however these systems have not been able to achieve the same temporal resolution as PDA-based systems. The CardioCCD-SMQ (RedShirt Imaging, Decatur, GA) currently offers a spatial resolution of 80x80 while achieving a temporal resolution of 2000 frames per second (fps). The CCD camera may achieve higher temporal resolution and/or higher signal-to-noise ratios by a process known as "binning," however this process decreases the spatial resolution of the camera, the major advantage of CCD technology. When using the CCD camera for cardiac mapping experiments, light saturation of the detector may be an issue and thus gain must be carefully controlled. Typically this is less of a problem with PDA systems. The basis of operation of the CCD detector is a shift registration process. Charge which is accumulated due to photons falling upon light-sensitive regions within the detector is transferred along the 2-dimensional detector array until the charge within a given potential well reaches the final readout electrode. The transfer of charge is accomplished by changing the voltage in an adjacent pixel, causing electrical charge to flow in the desired direction.

Although more costly than either CCD cameras or PDAs, the CMOS camera boasts exciting technology that has recently become capable of delivering extremely high spatiotemporal resolution. RedShirt Imaging lists the CardioCMOS-128f as being capable of recording 128x128 spots at an acquisition rate of 10,000 fps (RedShirt Imaging, LLC, Decatur, GA). CMOS technology typically allows for a very large well depth and a large dynamic range, although these cameras still lack the DC coupling ability of the PDA system. The architecture of the CMOS detector is what sets it apart from the CCD detector. The CMOS detector uses specialized manufacturing techniques to create micro-arrays of photodetectors, each with their own dedicated amplifiers and independent circuitry. Thus CMOS detectors are capable of performing signal processing functions on a pixel-by-pixel basis. The ability of the CMOS detector pixel to record and process signals on a pixel-by-pixel basis is in contrast to the CCD detector, which must transfer signals from individual pixels to be processed by downstream electrical circuitry. This fundamental difference in

circuitry architecture is reflected in the higher acquisition rates typically observed in CMOS detectors.

The PDA, as well as the individual photodiode, remains a cost-effective and rugged solution to a wide variety of problems within the field of COM. Photodiode arrays boast a wide spectral response, high dynamic range, high temporal resolution, and the largest well depth of the COM detectors. The PDA is typically a rugged device and can operate in high-light conditions typical in most laboratory experiments, while still delivering a high signal-to-noise ratio. Although low-light conditions can be achieved in COM applications, this typically places limitations on ΔF/F. Another interesting and unique feature of the PDA as a COM detector is that they may be AC coupled. This removal of the DC component of the signal allows the entire dynamic range of the detector to be used on the signal itself, rather than on both the signal and the background baseline fluorescence. This is particularly helpful when imaging with dyes that have a large background fluorescence signal (e.g., di-4-ANEPPS). Due to their robust nature and versatility in a wide variety of applications, photodiode-based systems remain the "workhorse" detector in COM. The PDA operates on principles based on the individual photodiode. Currents from individual photodiodes in the PDA are converted into voltages, which are read out of the detector in parallel and processed by a PC.

The typical noise levels, sensitivity, speed, spatial resolution, and ability to respond to high light levels without saturation (i.e. well depth) are summarized in the following table:

	Noise Levels	Sensitivity	Speed	Spatial Resolution	Well Depth
CCD	**	****	**	****	**
CMOS	****	***	****	*****	****
PDA	*****	****	*****	**	*****
PMT	***	*****	*****	*	**

Table.

For the above chart, more asterisks means better performance, which in the case of COM translates into lower noise, greater sensitivity, greater speed, higher spatial resolution, and a larger well depth. A few caveats apply to the above chart. Although the PMT has extraordinary speed and sensitivity, it is limited by the fact that there is typically no spatial resolution, and must be used in a sequential scanning method. Also, the authors have tried to take into account the *useful* range of a particular characteristic of the detector. For example, many CCD cameras are capable of recording at a rate of 2 kHz, however in practice it is currently challenging to obtain useful signals (S/N > 5) at this rate and at full spatial resolution. Rates of 200-500 Hz are more typical in practice. Also, it must be mentioned that these technologies are constantly and rapidly evolving, thus these ratings are of course subject to change. Also, note that the above comparisons refer to detectors commonly used in COM, and are not meant to serve as a basis for comparison for these technologies in general.

2.3 Filtration, digitization, and multiplexing

Optical signals are subject to several types of noise which must be removed in order to accurately study the details of the cardiac AP. We will briefly review the types of noise most relevant to COM systems. Various types of white noise are ubiquitous throughout all types

of electronics, and are typically of frequencies well above those of cardiac signals. Thus low pass filters are typically used to help remove white noise. Sixty-cyle is another type of noise that is often encountered when collecting optical signals. This noise may contaminate signals by way of electromagnetic waves from nearby power outlets, or may be introduced if equipment used in optical mapping experiments is powered using AC power (i.e., if the equipment is not isolated). It may be alleviated by the use of a Faraday cage and/or the use of a band-stop (i.e., notch) filter centered at 60-Hz. Mechanical vibrations may also affect optical signals, and can range from fluctuations in air current to vibrations due to foot traffic. Sources of mechanical vibrations are highly varied in nature, and must be dealt with on a case-by-case basis. A research-grade optical table with active isolation should be sufficient to suppress most sources of mechanical noise. Optical recordings may also contain drifts in basline voltage due to several sources. These include photobleaching, dye washout, and dye internalization into the inner leaflet of the cell membrane. One way to reduce the impact of these noise sources is to employ the technique of ratiometry (Knisley et al., 2000), which is discussed in the *Pre/Post-Conditioning* section which follows.

Many optical devices, including photodiodes and photomultiplier tubes, record analog signals that must be digitized before being stored on a PC. Digitization equipment must have sufficient speed and throughput in order to follow the high spatiotemporal resolution required for optical mapping applications. A review article by Entcheva et al. summarizes the state of the art in this sub-field of COM (Entcheva & Bien, 2006).

When data is recorded from a two-dimensional grid of sites simultaneously, the most intuitive storage method is a two-dimensional matrix of values. However, prior to storage on a PC, this data must be routed from the digitization equipment to the PC. This requires arranging the data in a sequential fashion, a process known as multiplexing. For a 16x16 element PDA, data for a single millisecond might be arranged from sites 1 to 256 and then be sequentially sent to the PC for storage. Following this, the data could then be demultiplexed and arranged as a 2D matrix, a more logical form for creating activation maps and other graphics to assist with visualization of the data.

2.4 Pre/post-conditioning of optical data

In contrast to electrical signals, optical signals are highly sensitive to heart motion. Various methods have been developed in order to reduce "motion artifacts" which are often present in optical signals. These motion artifacts are thought to be the result of a change in the location of the mapped region on the heart surface, where a fluorescence gradient typically exists (Himel & Knisley, 2006). Methods to reduce motion artifact include physically restraining the heart (Efimov et al., 1996; Girouard et al., 1996), the use of electromechanical uncouplers (Federov et al., 2007; Jalife et al., 1998; Li & Nattel, 2007; Wu et al., 1998), and the technique of ratiometry (Hooks et al., 2001; Knisley et al., 2000; Kong et al., 2003). Physically restraining the heart reduces motion artifacts simply by limiting the extent to which the heart can move during contraction, thus limiting the amount by which the mapped region moves with respect to its original position on the heart. Electromechanical uncouplers work by a variety of methods, but most have an effect upon the actin-myosin cytoskeleton which is responsible for contraction. Electromechanical uncouplers should be used with care, as some studies have shown that these agents can affect various parameters of the cardiac AP and may also affect the dynamics of ventricular fibrillation (VF) (Baker et al., 2004; Biermann et al., 1998; Hyashi et al., 2003; Lee et al., 2001).

Ratiometry is a signal processing method that requires the use of two recorded optical signals, each of a different band of the wavelength spectrum. We will refer to the longer wavelength signal as "red" and the shorter wavelength signal as "green". When the V_m-sensitive dye di-4-ANEPPS is excited, the peak of the emission spectrum of the dye shifts toward shorter wavelengths (green). Thus the green signal would show an increase in fluorescence intensity while the red signal would show a corresponding decrease in intensity. Using this method, an upright cardiac AP would be recorded in the green signal while an inverted (or "upside-down") AP would be recorded in the red signal. The important thing to consider is that the emission signal corresponding to V_m is emitted at a relatively narrow frequency band. Contrastingly, emission due to motion is not heavily wavelength-dependent, and will cause the change in fluorescence signals in the same direction regardless of the wavelength band of the collected signal. Since the motion signals are common to both collected wavelengths, we may reduce motion artifacts by simply taking the ratio of the green signal to the red on a point-by-point basis. This will cause a significant reduction in the motion artifact, and will help us to isolate the electrical signal. This technique could be achieved in the laboratory by using dual PDAs and separating fluorescence emission into two wavelength bands, one above and one below the peak emission wavelength of the dye of interest. In addition to motion artifact removal, ratiometric signals have also been used to study motion artifacts optically. This may be achieved by subtracting the electrical signal from the signal containing both electrical and motion components (Himel et al., 2006).

Since fibrillation (both ventricular and atrial) is a topic of great clinical and theoretical interest, considerable effort has been expended in order to analyze data recorded from the fibrillating heart. This data is challenging to analyze and interpret, since recordings of fibrillation often have a chaotic appearance when viewed with time as the horizontal axis. Thus a variety of alternate methods have been used to gain insight into the nature of fibrillation, including dominant frequency analysis (Caldwell et al., 2007; Choi et al., 2003; Choi et al., 2006; Joel & Hsia, 2005; Moreno et al., 2005; Wu et al., 2004; Wu et al., 2006; Zaitsev et al., 2003) and mutual information (Omichi et al., 2004, Wu et al., 2005). More recently the use of a metric known as spatiotemporal entropy has been used to analyze oscillatory dynamics in cardiac and neural systems (Bub et al., 2005; Jung et al., 2000; Himel et al., 2009).

Dominant frequency analysis involves use of the Fourier transform to examine the frequency content of fibrillation recordings. Some groups have used dominant frequency analysis to support the theory of a "mother rotor" (i.e., a high-frequency region of the heart that drives fibrillatory activity) (Chen et al., 2000; Jalife et al., 1998; Zaitsev et al., 2000), however this issue remains controversial (Berenfeld et al., 2001). Others believe that fibrillation is maintained by the constant creation and annihilation of wavelets which occur due to functional and anatomical heterogeneities (Choi et al., 2002; Lee et al., 1996; Moe, 1962; Rogers et al., 1999; Valderrábano et al., 2002). More recently, some groups have concluded that fibrillatory activity may be driven by both mechanisms, depending on specific conditions in the heart (Chen et al., 2003; Liu et al., 2004; Nash et al., 2006; Wu et al., 2002).

Mutual information techniques have been used to examine the relationship between V_m and Ca_i. Algorithms assign a numerical value for individual signals in order to quantify the degree of similarity between V_m and Ca_i during fibrillation in order to give insight into the mechanisms of arrhythmogenesis and the maintenance of fibrillation; however, mutual information must be calculated for individual signal pairs and by itself does not indicate *spatiotemporal* heterogeneities in V_m/Ca_i relationships.

Spatiotemporal entropy has been used to quantify the degree of uncertainty in both time and space by considering them as lumped parameters, and analyzing activations in the context of space-time cubes (i.e., stacked two-dimensional optical maps with time as the third dimension). Spatiotemporal entropy has been used to analyze neural simulations as well as oscillatory dynamics in cultured cell monolayers (Bub et al., 2005; Jung et al., 2000). Spatiotemporal entropy analysis is appealing when analyzing optical mapping data, since one of the main strengths of COM data lies in its spatial resolution.

3. Studies in cardiac electrophysiology research using photodiode arrays

This section will showcase three recent optical mapping studies from this lab which examine cardiac arrhythmia mechanisms in the context of global ischemia (Himel et al., 2009; Lakireddy et al., 2005; Lakireddy et al., 2006). These studies examine the dynamic relationship between V_m and Ca_i over the course of ischemia/reperfusion injury. These studies used a photodiode-based system which simultaneously records V_m and Ca_i with two separate 16x16 PDAs (figure 2 shows 16x16 element photoactive region of the PDA, see figure 3 for a schematic of the simultaneous dual-measurement system). This system was designed by B.R. Choi and G. Salama, and uses two Hamamatsu C4675-103 detectors. Please see the excellent review by Salama et al. for more details regarding this system (Salama et al., 2009). The whole-heart guinea pig (GP) Langendorff model was used, where the aorta was cannulated and hung vertically within a surrounding bath of physiological solution referred to as Tyrode's solution. Heated (~37° C), oxygenated Tyrode's solution was pumped retrogradely through the aorta in order to nourish and oxygenate the heart via the coronary arteries. These studies simulated the condition of global ischemia (i.e., oxygen deprivation) and reperfusion by temporarily interrupting perfusion into the coronary arteries and then restarting the perfusion. The guinea pig animal model is similar to human physiology in terms of its AP morphology and intracellular calcium handling.

Study 1 (Himel et al., 2009): Ventricular tachycardia is frequently observed in the clinical environment. VT may either be brief (<30 seconds) or may continue indefinitely, and patient survival is critically dependent on the duration of the VT episode. Spontaneous termination of the VT episode within a few seconds leaves the patient unharmed. If the VT episode continues however, the patient is typically dependent upon a defibrillatory shock to terminate the episode, without which the patient may not survive. Although extremely important clinically, the mechanism which determines the duration of the VT episode is not well understood. It is thought that uncoupling between V_m and Ca_i coupling may play a role in determining whether an episode of VT will terminate spontaneously or continue indefinitely. This study sought to use the concept of spatiotemporal entropy (E) as a metric to determine the degree of uncoupling between V_m and Ca_i during the early phases of a VT episode, and to test the predictive power of E for VT duration. During normal sinus rhythm, propagation of excitation waves in the heart is uniform and wavebreak is typically not observed. During episodes of VT, wavebreak is common, and fragmentation of excitation waves in the heart is frequently observed. Moreover, differences between V_m and Ca_i signals are often observed. These differences in V_m/Ca_i coupling may be quantified using the absolute value of the difference in E, symbolized by E_d.

This study examined several groups of VT episodes which were divided according to whether or not they terminated spontaneously. Self-terminating episodes of VT were further classified as short (<5 seconds) or long (>5 seconds). E_d was determined for the first 500 ms

of all VT episodes. E_d values for non self-terminating episodes of VT were significantly greater than self-terminating VT episodes. Further, E_d values for long self-terminating episodes of VT were significantly greater than those for short self-terminating episodes.

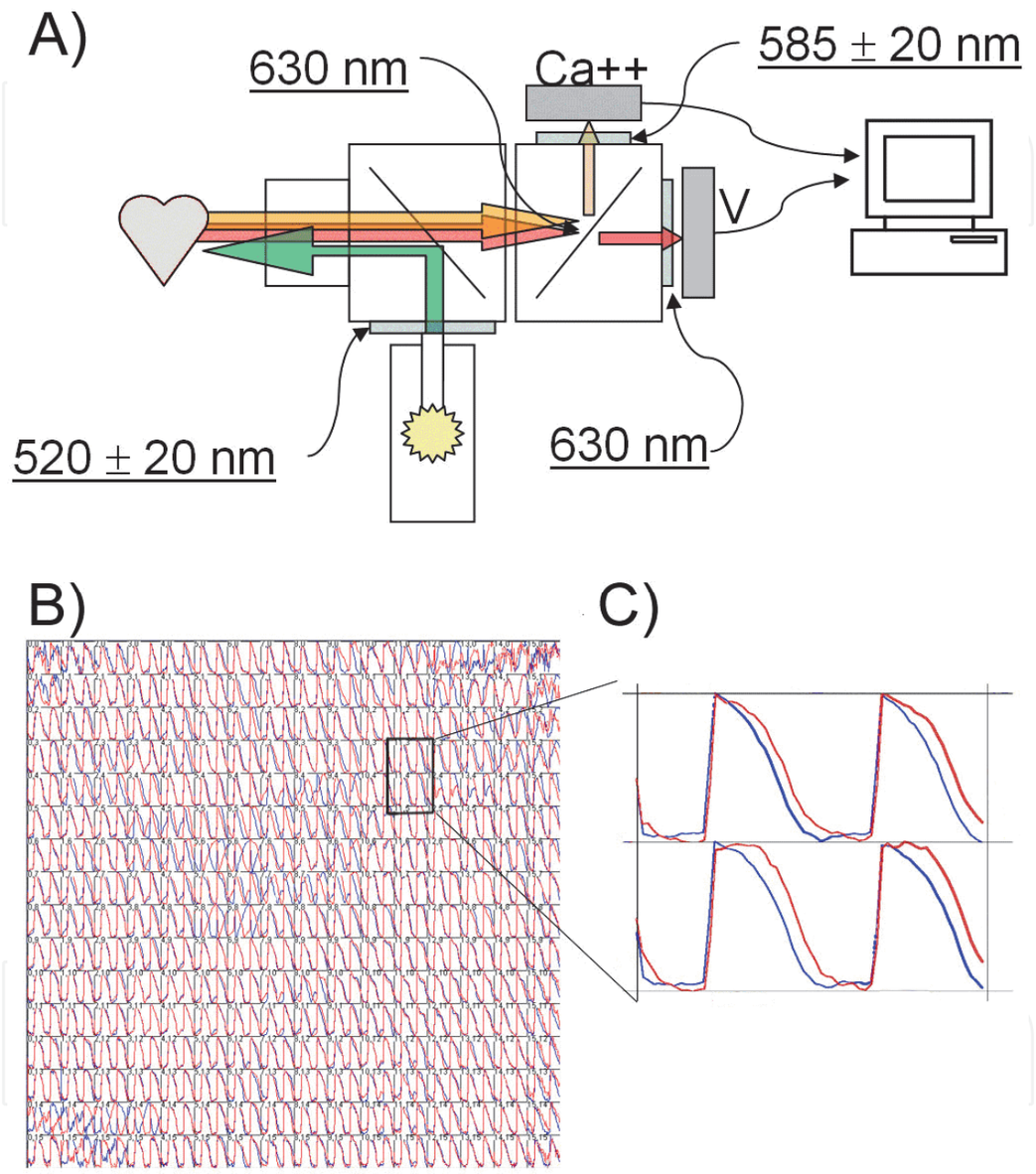

Fig. 3. Optical mapping diagram for simultaneous V_m and Ca_i measurements. For panel A), the position of each filter is indicated by thin curved lines with arrowheads, and the characteristics of the filters are underlined (high pass filters are indicated by a single number, whereas band pass filters have number ± band). The calcium and voltage PDAs are shaded gray. The large color-filled lines indicate the path of the given color of light. The excitation source is the bottom component in panel A). Panel B) shows an map of optical signals, and panel C) shows enlarged traces of the indicated pixels. The blue signal in panel C) represents V_m, whereas the red signal indicates Ca_i.

Wavebreak and differences in V_m and Ca_i spatial fluorescence maps were consistently identified during periods of high E and high E_d. The results are illustrated by figures 4 and 5, which show typical examples of low and high E_d during VT episodes.

High E_d correlated with a greater duration of a VT episode. This may be related to destabilization of propagation and uncoupling between V_m and Ca_i activation wavefronts.

Study 2 (Lakireddy et al., 2005): This study examines spatial dispersion of repolarization in the context of global ischemia, and also the role spatial dispersion plays in the development of electrical alternans. Electrical alternans is a term used to describe beat-to-beat alterations in AP morphology. For example, a one-to-one APD alternans occurs when a normal AP is followed by a short-duration AP, which is then followed by normal AP, short-duration AP, and so on. Electrical alternans are considered to be a strong marker of electrical instability, and often precede malignant arrhythmias such as ventricular tachycardia (VT) and VF (Hohnsloser et al., 1998; Gold et al., 2000; Ikeda et al., 2006; Pastore et al., 1999; Pham et al., 2003; Rashba et al., 2004; Rosenbaum et al., 1994).

In this study by Lakireddy et al., ischemia-induced changes in APD and intracellular calcium transient duration (Ca_iT-D) were determined, and their relationship with electrical alternans was investigated. Recordings show that ischemia resulted in a significant decrease in APD, but resulted in a significant increase in Ca_iT-D. In addition, changes in APD were spatially heterogeneous while changes in Ca_iT-D were relatively homogeneous (see figure 6). Sites with less shortening of APD displayed alternans in both Ca_iT-D and APD, while sites with more shortening of APD displayed Ca_iT-D alternans but little or no APD alternans, leading to a condition of significant spatial dispersion of the APD. The condition of increased spatial dispersion due to ischemia is thought to account for the vulnerability of the heart to alternans.

Study 3 (Lakireddy et al., 2006): In a second study by Lakireddy et al., the association between arrhythmogenesis and spontaneous calcium oscillations (S-CaOs) was examined in the intact heart. It is known that ischemia/reperfusion leads to elevated Ca_i and an alteration in Ca_i kinetics (Bers, 2002; Marban et al., 1990; Steenbergen et al., 1987). This alteration in normal Ca_i kinetics can lead to S-CaOs. Under such conditions, the normal master/slave relationship between V_m/Ca_iT signals is reversed (i.e., calcium signals precede and drive V_m).

The goal of this study was to investigate the correlation between S-CaOs and arrhthmogenesis using an experimental GP model with 15 minutes of no flow ischemia followed by 15 minutes of reperfusion. Changes in Ca_i and Vm in a limited zone of the epicardial surface of the GP heart were simultaneously recorded and carefully examined. The study provided evidence of a linkage between S-CaOs and arrhythmogenesis in the setting of ischemia/reperfusion (I/R). In the intact heart during I/R, spontaneous premature beats (PBs) occurred and were ubiquitous. Some PBs initiated a VT or VF (see figure 7), while others remained confined to their site of origin and did not result in an arrhythmia (see figure 8). Two important observations had to be made in order to link an arrhythmia to S-CaOs in the experimental model. First, the beginning of S-CaOs preceded the onset of the simultaneously recorded membrane depolarization by 2-15 ms at a very restricted site in the optical field. In recordings obtained further away from the focal site of origin, the relative amplitude of the S-CaOs gradually decreased and the start of membrane depolarization preceded the onset of S-CaOs. Second, the presence of some degree of conduction block, which by definition is the failure of S-CaOs to trigger a fully propagated

response, was essential for the localization of the focal site of origin. Thus S-CaOs may remain concealed (and hence benign) or may manifest as PBs, VT or VF.

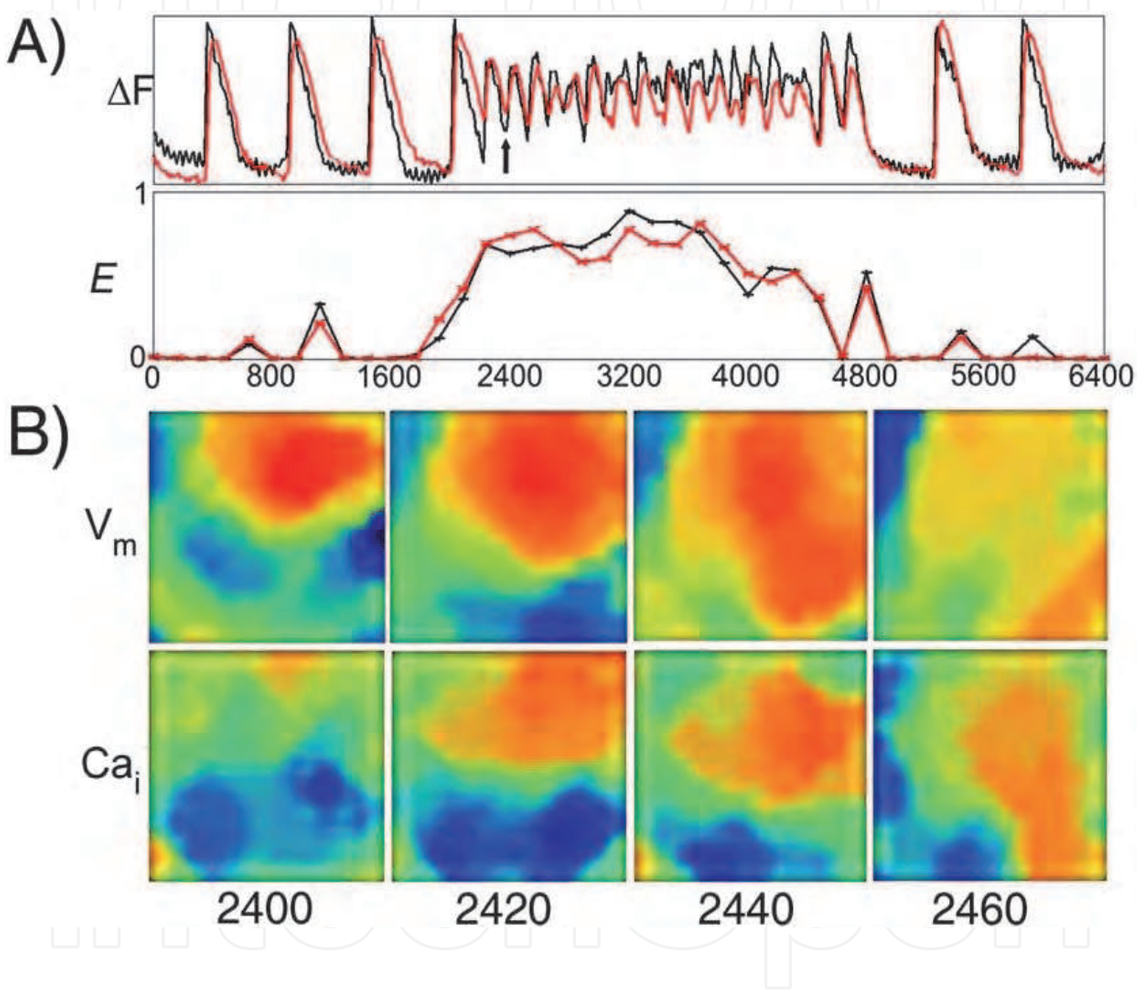

Fig. 4. Example of spatiotemporal entropy from a short self-terminating run of a ventricular tachyarrhythmia. V_m and Ca_i were recorded using a dual PDA system. Entropy traces (2nd row, panel A) show small differences between V_m and Ca_i entropy, indicating a low degree of spatiotemporal uncoupling. Fluorescence maps in panel B show similar, but not identical excitation wavefronts for V_m and Ca_i. Values given for traces and fluorescence maps are given in ms. (*reproduced with permission from Himel et al., 2009*).

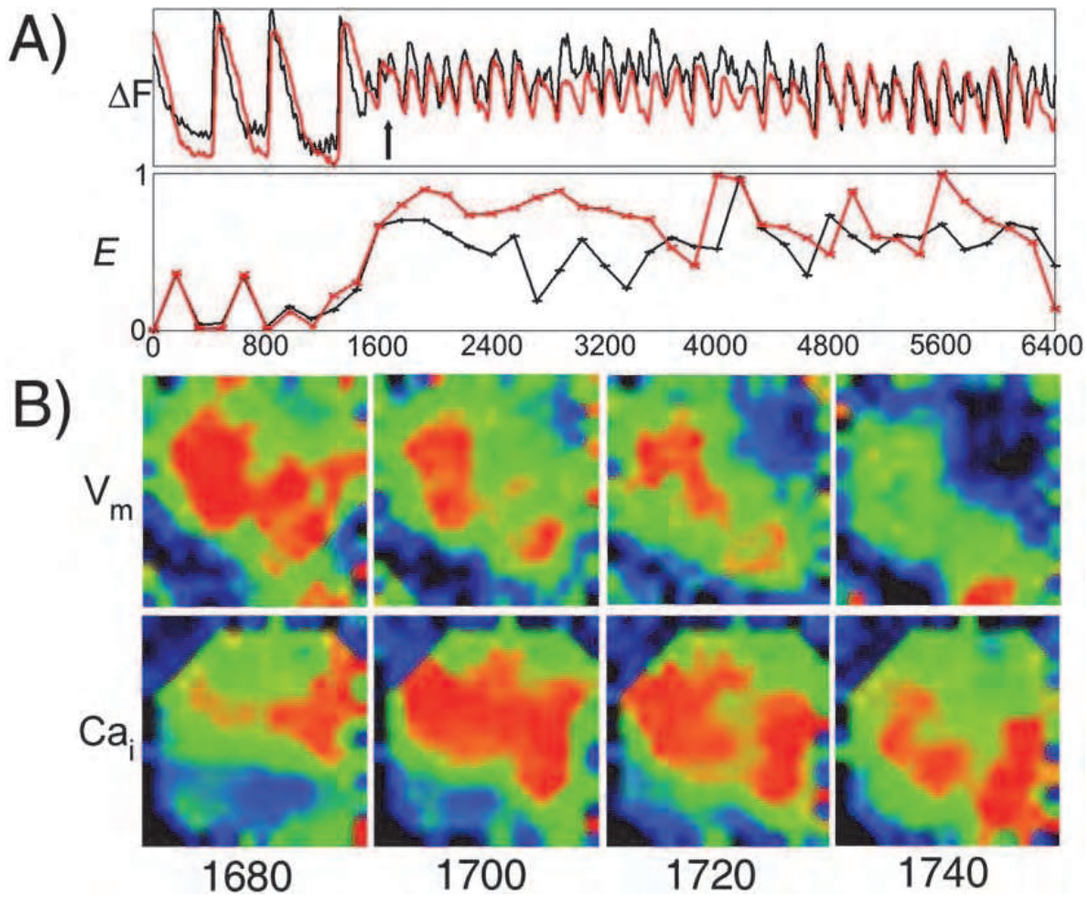

Fig. 5. Example of spatiotemporal entropy from a non self-terminating run of a ventricular tachyarrhythmia. Differences in the entropy traces (2nd row, panel A) show a disparity between V_m and Ca_i entropy and spatiotemporal uncoupling. Spatial fluorescence maps reflect the disparity shown by the V_m and Ca_i traces. Values given for traces and fluorescence maps are in ms. (*reproduced with permission from Himel et al., 2009*).

4. Recent advances in cardiac optical mapping

We will now turn to briefly discuss a few of the important recent advances in COM. Optrodes are bundles of microscopic fiberoptic cables which are inserted into cardiac tissue in order to interrogate intramural activation patterns. They are similar to plunge needle electrodes in their usage; however optrodes are capable of measuring complete APs, including the repolarization phase, whereas plunge electrodes measure extracellular potentials only. It is thought that in the future optrodes will play an important role in more carefully examining transmural dispersion of repolarization, an important factor in arrhythmogenesis in a variety of cardiac diseases (Antzelevitch, 2007; El-Sherif et al., 1996; Milberg et al., 2005; Shimizu et al., 1997). Optrodes may also be important in the study of the dynamics of arrhythmic circuits, since they are often present deeper in the myocardial wall (Allison et al., 2007; Li et al., 2008; Valderrábano et al., 2001). However, like plunge electrodes optrodes must also be inserted into the tissue and therefore cause damage which may by itself alter activation patterns. Thus the effects of this insertion must be carefully

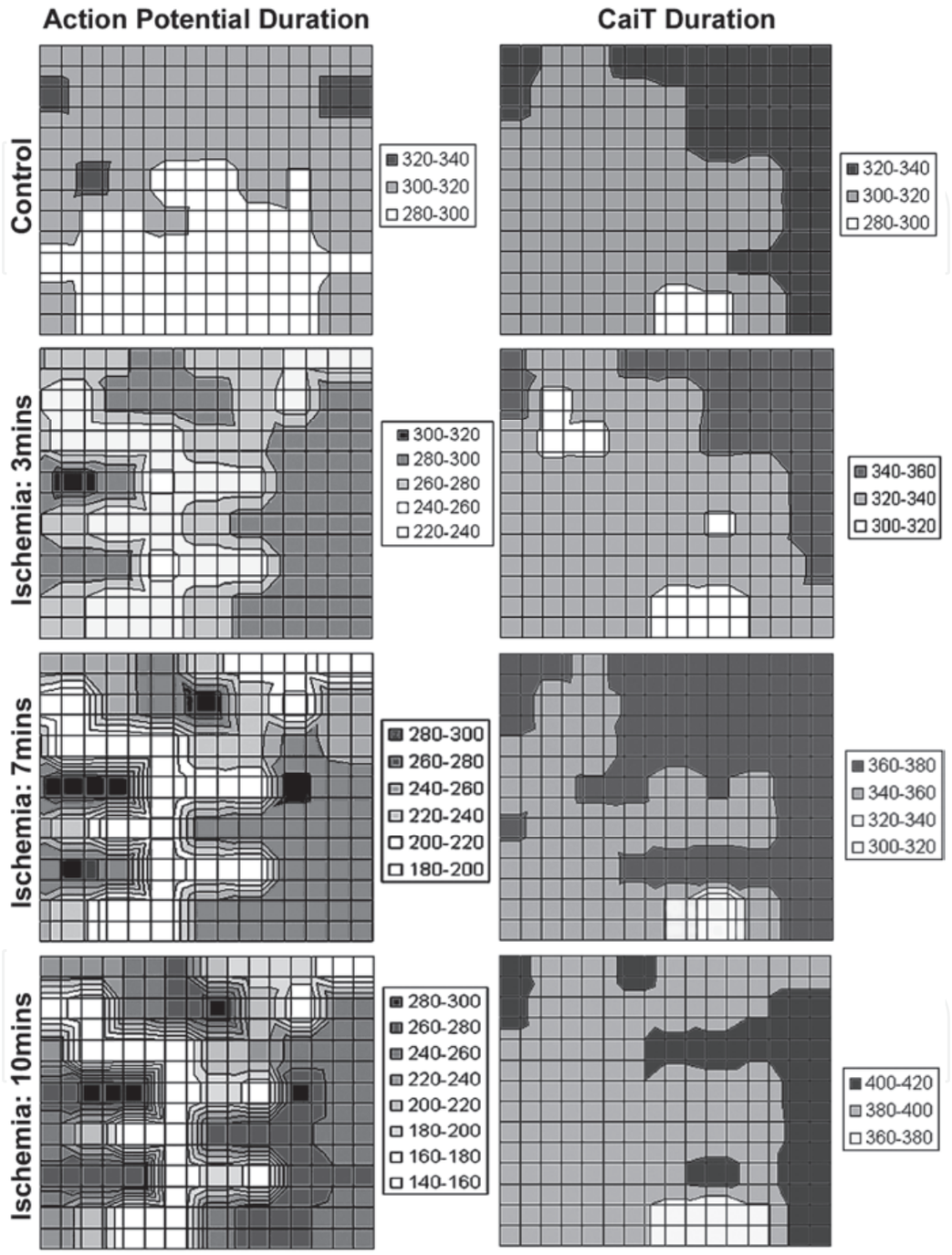

Fig. 6. APD and Ca_iT-D during normal perfusion and into ischemia. Scales to the right indicate the color of a given APD or Ca_iT-D. *(reproduced with permission from Lakireddy et al., 2005).*

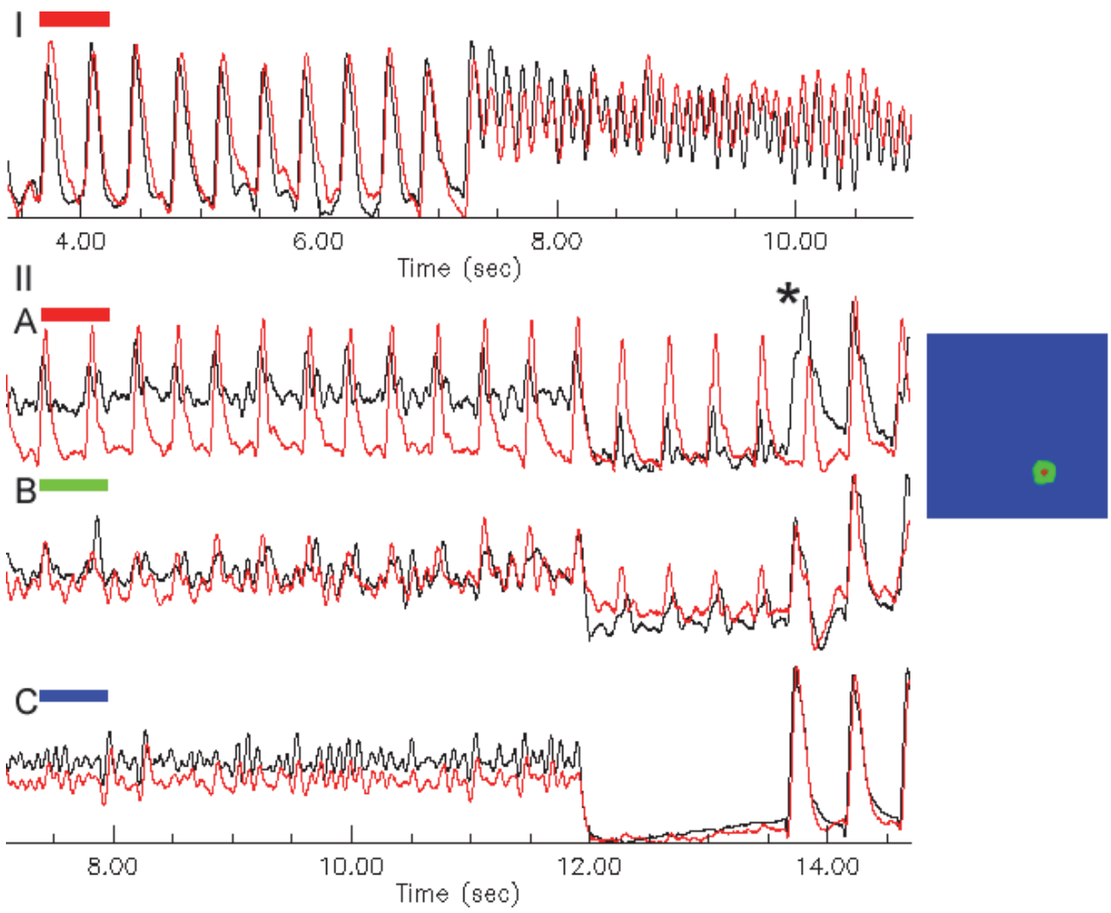

Fig. 7. Concealed spontaneous calcium oscillations (S-CaOs). Recordings were obtained from an experiment in which localized S-CaOs developed during an episode of self-terminating VF and continued uninterrupted after the resumption of spontaneous cardiac rhythm. Panel I illustrates the initiation of VF. Panel II shows recordings from three representative pixels (marked by different colors in the map of the optical field, seen to the right of the traces). After the self-termination of VF (at approximately 12 seconds), the majority of the optical field showed a pause with no electrical activity (trace C of panel II), while the localized S-CaOs continued. *(reproduced with permission from Lakireddy et al., 2006).*

considered when interpreting intramural data (El-Sherif, 2007). Photodiodes have played a dominant role in the construction of optrodes (Caldwell et al., 2005; Kong et al., 2007; Byars et al., 2003).

Several groups have recently begun to use multiple cameras to simultaneously interrogate opposing sides of the ventricular wall (Evertson et al., 2008; Kay & Rogers, 2006; Kay et al., 2004; Kay et al., 2006; Rogers et al., 2007). In addition, some of these groups use additional cameras to recreate the geometry of the heart in order to properly orient optical maps from several cameras on the epicardial surface (Kay et al., 2004; Evertson et al., 2008). Most Panoramic optical mapping systems are based on CCD technology, however systems have also been built using multiple PDAs (Qu et al., 2007). Panoramic optical mapping does not address the problem of lost depth information, but does provide a significant improvement over traditional optical mapping which only maps a limited region on the epicardial surface.

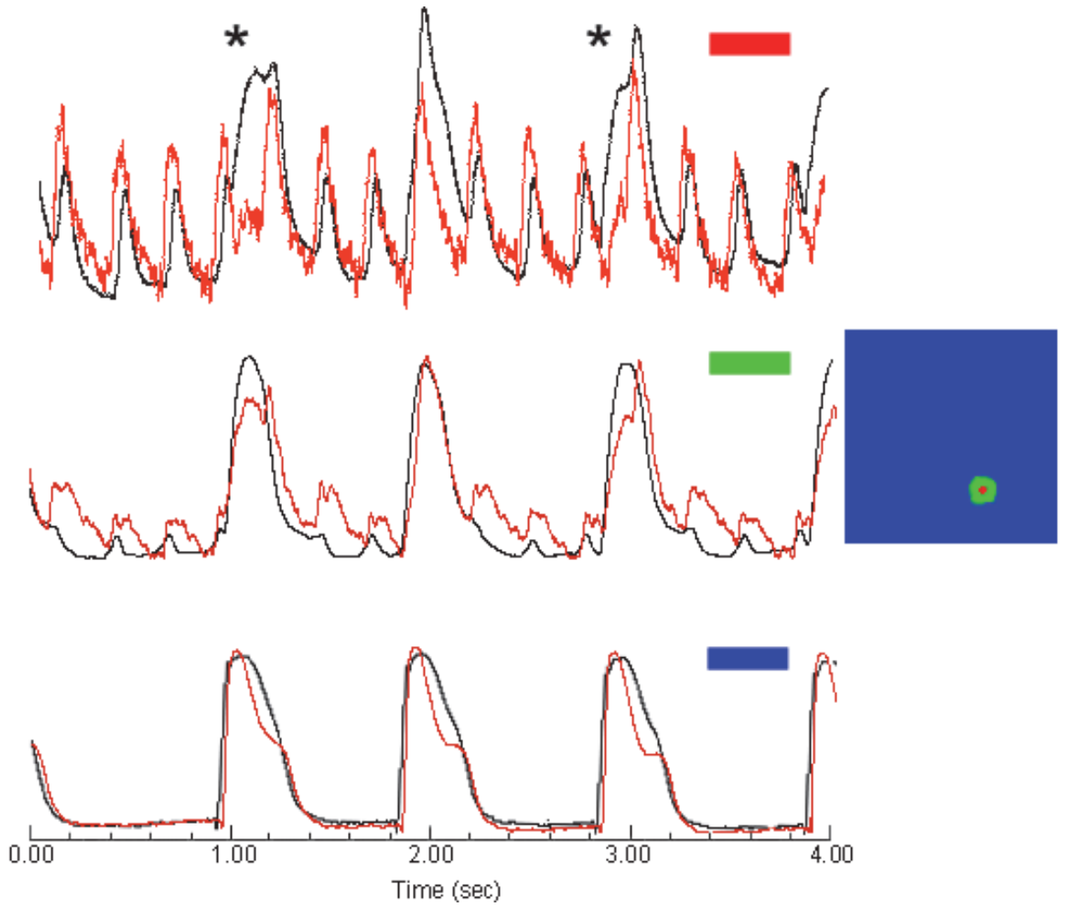

Fig. 8. Calcium oscillations confined to a site within the mapping field. The top, middle, and bottom traces show recordings from the red, green, and blue regions of the mapping field, respectively. The top trace shows regular calcium oscillations driving V_m. The middle trace shows the presence of calcium oscillations which are significantly depressed with respect to those in the top trace, and do not precede V_m. The bottom row shows that the calcium transients are being driven by voltage, implying that the calcium oscillations in the red region of the map have failed to escape the red/green region of the map and propagate through to the blue region. *(reproduced with permission from Lakireddy et al., 2006).*

The use of monolayer cell cultures in COM also represents an important advance, allowing for highly controlled studies of basic conduction as well as studies to elucidate fundamental arrhythmic mechanisms (Bub et al., 1998; Entcheva et al., 2000; Fast et al., 2000; Iravanian et al., 2003; Tung & Cysyk, 2007). An appealing aspect of the cardiac monolayer is that it allows us to study conduction in cardiac tissue without the complexity associated with the three-dimensional whole-heart Langendorff model. Since the cardiac monolayer is essentially two-dimensional (only tens of micrometers thick while being tens of millimeters in diameter), the entire monolayer may be mapped; therefore data interpretation is not complicated by the absence of missing depth information. And although the monolayer is technically three-dimensional, typical optical mapping systems interrogate at sufficient depths so that no information is lost beneath the surface (Ding et al., 2001). Despite being similar to whole-heart mapping in many respects, the actual practice of monolayer mapping

carries with it significant challenges, and is in many respects more difficult than whole-heart mapping (Entcheva & Bien, 2006).

5. Conclusion

Photodiodes have played an essential role in the development of the field of COM. They were used in the earliest COM systems and continue to have widespread use today, both in typical applications as well as more modern designs such as optrodes and panoramic systems. Applications for photodiodes within COM continue to emerge, and will likely remain a vital part of this important and ever-expanding branch of cardiac electrophysiology research.

6. List of abbreviations

AP – action potential
AP-A – anthopleurin-A
APD – action potential duration
Ca_i – intracellular calcium
Ca_iT – intracellular calcium transient
Ca_iT-D – intracellular calcium transient duration
CCD - charge-coupled device
CL – cycle length
CMOS - complimentary metal-oxide semiconductor
COM – cardiac optical mapping
GP – guinea pig
I/R – ischemia/reperfusion
LQTS – long QT syndrome
LQT3 – long QT syndrome 3
PB – premature beat
PDA - photodiode array
PMT - photomultiplier tube
TdP – Torsades de Pointes
VF – ventricular fibrillation
V_m – transmembrane voltage
VT – ventricular tachycardia

7. References

Allison JS, Qin H, Dosdall DJ, Huang J, Newton JC, Allred JD, Smith WM, Ideker RE. The transmural activation sequence in porcine and canine left ventricle is markedly different during long-duration ventricular fibrillation. J Cardiovasc Electrophysiol 2007;18:1306-1312.

Al-Khadra A, Nikolski V, Efimov IR. The role of electroporation in defibrillation. Circ Res 2000;87:797-804.

Antzelevitch C. Role of spatial dispersion of repolarization in inherited and acquired sudden cardiac death syndromes. Am J Physiol Heart Circ Physiol 2007;293:H2024–H2038.

Baker LC, Wolk R, Choi BR, Watkins S, Plan P, Shah A, Salama G. Effects of mechanical uncouplers, diacetyl monoxime, and cytochalasin-D on the electrophysiology of perfused mouse hearts. J Physiol Heart Circ Physiol 2004;287:H1771-H1779.

Baxter WT, Mirinov SF, Zaitsev AV, Jalife J, Pertsov AM. Visualizing excitation waves inside cardiac muscle using transillumination. Biophys J 2001;80:516-530.

Berenfeld O, Pertsov AM, Jalife J. Letter to the editor: What is the organization of waves in ventricular fibrillation. Circ Res 2001;89:e22.

Bers DM. Calcium and cardiac rhythms: physiological and pathophysiological. Circ Res 2002;90:14-17.

Biermann M, Rubart M, Moreno A, Wu J, Josiah-Durant A, Zipes DP. Differential effects of cytochalasin D and 2,3 butanedione monoxime on isometric twitch force and transmembrane action potential in isolated ventricular muscle: implications for optical measurements of cardiac repolarization. J Cardiovasc Electrophysiol 1998;9:1348-1357.

Bub G, Glass L, Publicover NG, Shrier A. Bursting calcium rotors in cultured cardiac myocyte monolayers. Proc Natl Acad Sci USA 1998;95:10283-10287.

Bub G, Shrier A, Glass L. Global organization of dynamics in oscillatory heterogeneous excitable media. Physical Review Lett 2005;94:028105.

Byars JL, Smith WM, Ideker RE, Fast VG. Development of an optrode for intramural multisite optical recordings of Vm in the heart. J Cardiovasc Electrophysiol 2003;14:1196-1202.

Cabo C, Pertsov AM, Baxter WT, Davidenko JM, Gray RA, Jalife J. Wave-front curvature as a cause of slow conduction and block in isolated cardiac muscle. Circ Res 1994;75:1014-1028.

Caldwell J, Burton FL, Smith GL, Cobbe ST. Heterogeneity of ventricular fibrillation dominant frequency during global ischemia in isolated rabbit hearts. J Cardiovasc Electrophysiol 2007;18:854-861.

Caldwell BJ, Legrice IJ, Hooks DA, Tai D, Pullan AJ, Smaill BH. Intramural measurement of transmembrane potential in the isolated pig heart: Validation of a novel technique. J Cardiovasc Electrophysiol 2005;16:1001-1010.

Chen J, Mandapati R, Berenfeld O, Skanes AC, Jalife J. High-frequency periodic sources underlie ventricular fibrillation in the isolated rabbit heart. Circ Res 2000;86:86-93.

Chen PS, Wu TJ, Ting CT, Karagueuzian HS, Garfinkel A, Lin SF, Weiss JN. A tale of two fibrillations. Circulation 2003;108:2298-2303.

Cheng Y. Optical mapping of shock-induced arrhythmogenesis in the rabbit heart with healed myocardial infarction: fluorescent imaging with a photodiode array. Methods Mol Med 2006;129:149-61.

Choi BR, Burton F, Salama G. Cytosolic Ca2+ triggers early afterdepolarizations and torsade de pointes in rabbit hearts with type 2 long QT syndrome. J Physiol 2002;543:615-631.

Choi BR, Hatton WJ, Hume JR, Liu T, Salama G. Low osmolarity transforms ventricular fibrillation from complex to highly organized, with a dominant high-frequency source. Heart Rhythm 2006;3:1210-1220.

Choi BR, Jang W, Salama G. Spatially discordant voltage alternans cause wavebreaks in ventricular fibrillation. Heart Rhythm 2007; 4:1057–1068.

Choi BR, Liu T, Lavasani M, Salama G. Fiber orientation and cell-cell coupling influence ventricular fibrillation dynamics. J Cardiovasc Electrophysiol 2003;14:851-860.

Choi BR, Salama G. Simultaneous maps of optical action potentials and calcium transients in guineapig hearts: mechanisms underlying concordant alternans. J Physiol 2000;529:171-188.

Coraboeuf E, Weidmann S. Potentiels d'action du muscle obtenus à l'aide de microélectrodes intracellulaires. Présence d'une inversion de potential. CR Soc Biol (Paris) 1949;143:1360-1360.

Coraboeuf E, Weidmann S. Potentiels de repos et potentials d'action du muscle cardiaque, mesurés á l'aide d'électrodes intracellulaires. CR Soc Biol (Paris) 1949; 143:1329-1331.

Draper MH, Weidmann S. Cardiac resting and action potentials recorded with an intracellular electrode. J Physiol 1951;115:74-94.

Ding L; Splinter, R.; Knisley, S.B. Quantifying spatial localization of optical mapping using Monte Carlo simulations. IEEE Trans Biomed Eng 2001;48:1098-1107.

Efimov IR, Ermentrout B, Huang DT, Salama G. Activation and repolarization patterns are governed by different structural characteristics of ventricular myocardium: Experimental study with voltage-sensitive dyes and numerical simulations. J Cardiovasc Electrophysiol 1996;7:512-530.

El-Sherif N. The challenge of cardiac tridimensional mapping. Heart Rhythm 2007;4:1437-1440.

El-Sherif N, Caref EB, Yin H, Restivo M. The electrophysiological mechanism of ventricular arrhythmias in the long QT syndrome. Circ Res 1996;79:474-492.

Entcheva E, Bien H. Macroscopic optical mapping of excitation in cardiac cell networks with ultra-high spatiotemporal resolution. Progress in Biophysics and Molecular Biology 2006;92:232–257.

Entcheva E, Lu SN, Troppman RH, Sharma V, Tung L. Contact fluorescence imaging of reentry in monolayers of cultured neonatal rat ventricular myocytes. J Cardiovasc Electrophysiol 2000;11:665-676.

Evertson DW, Holcomb MR, Eames MDC, Bray MA, Sidorov VY, Xu J, Wingard H, Dobrovolny HM, Woods MC, Gauthier DJ, Wikswo JP. High-resolution high-speed panoramic cardiac imaging system. IEEE Trans Biomed Eng 2008;55:1241-1243.

Fast VG. Simultaneous optical imaging of membrane potential and intracellular calcium. J Electrocardiol 2005;38:107-112.

Fast VG, Ideker RE. Simultaneous optical mapping of transmembrane potential and intracellular calcium in myocyte cultures. J Cardiovasc Electrophysiol 2000;11:547-556.

Fast VG, Sharifov OF, Cheek ER, Newton JC, Ideker RE. Intramural virtual electrodes during defibrillation shocks in left ventricular wall assessed by optical mapping of membrane potential. Circulation 2002;106:1007-1014.

Fedorov VV, Kostecki G, Hemphill M, Efimov IR. Atria are more susceptible to electroporation than ventricles: Implications for atrial stunning, shock-induced arrhythmia and defibrillation failure. Heart Rhythm 2008;5:593-604.

Fedorov VV, Lozinsky IT, Sosunov EA, Anyukhovsky EP, Rosen MR, Balke W, Efimov IR. Application of blebbistatin as an excitation– contraction uncoupler for electrophysiologic study of rat and rabbit hearts. Heart Rhythm 2007;4:619-626.

Girouard SD, Pastore JM, Laurita KR, Gregory KW, Rosenbaum DS. Optical mapping in a new guinea pig model of ventricular tachycardia reveals mechanisms for multiple wavelengths in a single reentrant circuit. Circulation 1996;93:603-613.

Gold MR, Bloomfield DM, MD, Anderson KP, El-Sherif N, Wilber DJ, Groh WJ, Estes M, Kaufman ES, Greenberg ML, Rosenbaum DS. A comparison of T-wave alternans, signal averaged electrocardiography and programmed ventricular stimulation for arrhythmia risk stratification. JACC 2000;36:2247-2253.

Hayashi H, Miyauchi Y, Chou CC, Karagueuzian HS, Chen PS, Lin SF. Effects of cytochalasin D on electrical restitution and the dynamics of ventricular fibrillation in isolated rabbit heart. J Cardiovasc Electrophysiol 2003;14:1077-1084.

Himel IV, HD, Bub G, Yue Y, and El-Sherif N. Early voltage/calcium uncoupling predestinates the duration of ventricular tachyarrhythmias during ischemia/reperfusion. Heart Rhythm 2009;6:1359-1365.

Himel IV, HD, Dumas JH, Kiser AC, Knisley SB. Translesion stimulus-excitation delay indicates quality of linear lesions produced by radiofrequency ablation in rabbit hearts. Physiol. Meas. 2007;28:611–623.

Himel IV, H.D., Knisley, S.B. Imaging of cardiac movement using ratiometric and nonratiometric optical mapping: effects of ischemia and 2, 3-butaneodione monoxime. IEEE Trans Med Imaging 2006;25:122-127.

Hohnloser SH, Klingenheben T, Li YG, Zabel M, Peetermans J, Cohen RJ. T wave alternans as a predictor of recurrent ventricular tachyarrhythmias in ICD recipients: Prospective comparison with conventional risk markers. J Cardiovasc Electrophysiol 1998;9:1258-1268.

Hooks DA, LeGrice IJ, Harvey JD, Smaill BH. Intramural multisite recording of transmembrane potential in the heart. Biophys J 2001;81:2671-2680.

Hyatt CJ, Mirinov SF, Vetter FJ, Zemlin CW, Pertsov AM. Optical Action Potential Upstroke Morphology Reveals Near-Surface Transmural Propagation Direction. Circ Res 2005;97:277-284.

Ikeda T, Yoshino H, Sugi K, Tanno K, Shimizu H, Watanabe J, Kasamaki Y, Yoshida A, Kato T. Predictive value of microvolt T-wave alternans for sudden cardiac death in patients with preserved cardiac function after acute myocardial infarction. JACC 2006;48:2268-2274.

Iravanian S, Nabutovsky Y, Kong CR, Saha S, Bursac N, Tung L. Functional reentry in cultured monolayers of neonatal rat cardiac cells. Am J Physiol Heart Circ Physiol 2003;285:H449–H456.

Jalife J, Berenfeld O, Skanes A, Mandapati R. Mechanisms of atrial fibrillation: mother rotors or multiple daughter wavelets, or both? J Cardiovasc Electrophysiol 1998;9:S2-12.

Joel SE, Hsia PW. Discovery of gradient pattern in dominant frequency maps during fibrillation: implication of rotor drift and epicardial conduction velocity changes. J Electrocardiol 2005;38:159-165.

Jung P, Wang J, Wackerbauer R, Showalter K. Coherent structure analysis of spatiotemporal chaos. Physical Review E 2000;61:2095-2098.

Kay MW, Amison PM, Rogers JM. Three-dimensional surface reconstruction and panoramic optical mapping of large hearts. IEEE Trans Biomed Eng 2004;51:1219-1229.

Kay MW, Rogers JM. Epicardial rotors in panoramic optical maps of fibrillating swine ventricles. Conf Proc IEEE Med Biol Soc 2006;1:2268-2271.

Kay MW, Walcott GP, Gladden JD, Melnick SB, Rogers JM. Lifetimes of epicardial rotors in panoramic optical maps of fibrillating swine ventricles. Am J Physiol Heart Circ Physiol 2006;291:1935-1941.

Knisley SB, Baynham T. Line stimulation parallel to myofibers enhances regional uniformity of transmembrane voltage changes in rabbit hearts. Circ Res 1997;81:229-241.

Knisley SB, Hill BC. Effects of bipolar point and line stimulation in anisotropic rabbit epicardium: assessment of the critical radius of curvature for longitudinal block. IEEE Trans Biomed Eng 1995;42:957-966.

Knisley SB, Hill BC, Ideker RE. Virtual electrode effects in myocardial fibers. Biophys J 1994;66:719-728.

Knisley SB, Justice RK, Kong W, Johnson PL. Ratiometry of transmembrane voltage-sensitive fluorescent dye emission in hearts. Am J Physiol Heart Circ Physiol 2000; 279: H1421–H1433.

Knisley SB, Trayanova N, Aguel F. Roles of electric field and fiber structure in cardiac electric stimulation. Biophys J 1999;77:1404-1417.

Kong W, Fakhari N, Sharifov OF, Ideker RE, Smith WM, Fast VG. Optical measurements of intramural action potentials in isolated porcine hearts using optrodes. Heart Rhythm 2007;4:1430-1436.

Kong W, Walcott GP, Smith WM, Johnson PL, Knisley SB. Emission ratiometry for simultaneous calcium and action potential measurements with coloaded dyes in rabbit hearts: reduction of motion and drift. J Cardiovasc Electrophysiol 2003;14:76-82.

Lakireddy V, Baweja P, Syed A, Bub G, Boutjdir M, El-Sherif N. Contrasting effects of ischemia on the kinetics of membrane voltage and intracellular calcium transient underlie electrical alternans. Am J Physiol Heart Circ Physiol 2005; 288:400-407.

Lakireddy V, Bub G, Baweja P, Syed A, Boutjdir M, El-Sherif N. The kinetics of spontaneous calcium oscillations and arrhythmogenesis in the in vivo heart during ischemia/reperfusion. Heart Rhythm 2006;3:58-66.

Lan DZ, Pollard AE, Knisley SB. Optical mapping of Vm and Cai 2+ in a model of arrhythmias induced by local catecholamine application in patterned cell cultures. Eur J Physiol 2007;453:871–877.

Laurita KR, Singal A. Mapping action potentials and calcium transients simultaneously from the intact heart. Am J Physiol Heart Circ Physiol 2001;280: H2053–H2060.

Lee JJ, Kamjoo K, Hough D, Hwang C, Fan W, Fishbein MC, Bonometti C, Ikeda T, Karagueuzian HS, Chen PS. Reentrant wave fronts in wiggers' stage II ventricular fibrillation. Circ Res 1996;78:660-675.

Lee MH, Lin SF, Ohara T, Omichi C, Okuyama Y, Chudin E, Garfinkel A, Weiss JN, Karagueuzian HS, Chen PS. Effects of diacetyl monoxime and cytochalasin D on ventricular fibrillation in swine right ventricles. Am J Physiol Heart Circ Physiol 2001;280: H2689–H2696.

Li D, Nattel S. Pharmacological elimination of motion artifacts during optical imaging of cardiac tissues: Is blebbistatin the answer? Heart Rhythm 2007;4:627-628.

Li L, Jin Q, Huang J, Cheng KA, Ideker RE. Intramural foci during long duration fibrillation in the pig ventricle. Circ Res 2008;102:1256-1264.

Liu YB, Pak HN, Lamp ST, Okuyama Y, Hayashi H, Wu TJ, Weiss JN, Chen PS, Lin SF. Coexistence of two types of ventricular fibrillation during acute regional ischemia in rabbit ventricle. J Cardiovasc Electrophysiol 2004;15:1433-1440.

Marban E, Kitakaze M, Koretsune Y, Yue DT, Chacko VP, Pike MM. Quantification of $[Ca2+]_i$ in perfused hearts: critical evaluation of the 5F-BAPTA and nuclear magnetic resonance method as applied to the study of ischemia and reperfusion. Circ Res 1990;66:1255-1267.

Matiukas A, Mitrea BG, Pertsov AM, Wuskell JP, Wei M, Watras J, Millard AC, Loew LM. New near-infrared optical probes of cardiac electrical activity. Am J Physiol Heart Circ Physiol 2006;290: H2633–H2643.

Matiukas, A, Mitrea BG, Qin M, Pertsov AM, Shvedko AG, Warren MD, Zaitsev AV, Wuskell JP, Wei M, Watras J, Loew LM. Near-infrared voltage-sensitive fluorescent dyes optimized for optical mapping in blood-perfused myocardium. Heart Rhythm 2007;4:1441-1451.

Milberg P, Reinsch P, Wasmer K, Mönnig G, Stypmann P, Osada N, Breithardt G, Haverkamp W, Eckardt L. Transmural dispersion of repolarization as a key factor of arrhythmogenicity in a novel intact heart model of LQT3. Circ Res 2005;65:397-404.

Moe GK. On the multiple wavelet hypothesis of atrial fibrillation. Arch Int Pharmacodyn Ther 1962;140:183–188.

Morad M, Dillon S. A new laser scanning system for measuring action potential propagation in the heart. Science 1981; 214:453-456.

Morad M, Salama G. Optical probes of membrane potential in heart muscle. J Physiol 1979;292:267-295.

Moreno J, Zaitsev AV, Warren M, Berenfeld O, Kalifa J, Lucca E, Mironov S, Guha P, Jalife J. Effect of remodelling, stretch and ischaemia on ventricular fibrillation frequency and dynamics in a heart failure model. Cardiovasc Res 2005;65:158-166.

Nash MP, Mourad A, Clayton RH, Sutton PM, Bradley CP, Hayward M, Paterson DJ, Taggart P. Evidence for multiple mechanisms in human ventricular fibrillation. Circulation 2006;114:536-542.

Neunlist M, Tung L. Spatial distribution of cardiac transmembrane potentials around an extracellular electrode: Dependence on fiber orientation. Biophys J 1995;68:2310-2322.

Omichi C, Lamp ST, Lin SF, Yang J, Baher A, Zhou S, Attin M, Lee MH, Karagueuzian HS, Kogan B, Qu Z, Garfinkel A, Chen PS, Weiss JN. Intracellular Ca dynamics in ventricular fibrillation. Am J Physiol Heart Circ Physiol 2004;286: H1836–H1844.

Pastore JM, Girouard SD, Laurita KR, Akar FG, Rosenbaum DS. Mechanism linking T-wave alternans to the genesis of cardiac fibrillation. Circulation 1999;99:1385-1394.

Perez FJ, Wood MA, Schubert CM. Effects of gap geometry on conduction through discontinuous radiofrequency lesions. Circulation 2006;113:1723-1729.

Pham Q, Quan KJ, Rosenbaum DS. T-wave alternans: marker, mechanism, and methodology for predicting sudden cardiac death. J Electrocardiol 2003;36:75-81.

Pruvot EJ, Katra RP, Rosenbaum DS, Laurita KR. Role of calcium cycling versus restitution in the mechanism of repolarization alternans. Circ Res 2004;94:1083-1090.

Qu F, Ripplinger CM, Nikolski VP, Grimm C, Efimov IR. Three-dimensional panoramic imaging of cardiac arrhythmias in rabbit heart. J Biomed Opt. 2007;12:044019.

Rashba EJ, Osman AF, Macmurdy K, Kirk MM, Sarang SE, Peters RW, Shorofsky SR, Gold MR. Enhanced detection of arrhythmia vulnerability using T wave alternans, left ventricular ejection fraction, and programmed ventricular stimulation: A prospective study in subjects with chronic ischemic heart disease. J Cardiovasc Electrophysiol 2004;15:170-176.

Rogers JM, Huang J, Smith WM, Ideker RE. Incidence, evolution, and spatial distribution of functional reentry during ventricular fibrillation in pigs. Circ Res 1999;84:945-954.

Rogers JM, Walcott GP, Gladden JD, Melnick SB, Kay MW. Panoramic optical mapping reveals continuous epicardial reentry during ventricular fibrillation in the isolated swine heart. Biophys J 2007;92:1090-1095.

Rosenbaum DS, Jackson LE, Smith JM, Garan H, Ruskin JN, Cohen RJ. Electrical alternans and vulnerability to ventricular arrhythmias. N Engl J Med 1994;330:235-241.

Sakai T. Optical mapping analysis of the spatiotemporal pattern of experimental tachyarrhythmia in improved isolated rat atrium preparation. J Physiol Sci 2008;58:87-97.

Salama G. Merocyanine 540 as an optical probe of transmembrane electrical activity in the heart. Science 1976;191:485-487.

Salama G, Choi BR, Azour G, Lavasani M, Tumbev V, Salzberg BM, Patrick MJ, Ernst LA, Waggoner AS. Properties of new, long-wavelength, voltage-sensitive dyes in the heart. J. Membrane Biol 2005;208:125–140.

Salama G, Hwang SM. Simultaneous optical mapping of intracellular free calcium and action potentials from langendorff perfused hearts. Curr Protoc Cytom 2009; Chapter 12: Unit 12.17.

Sano T, Ohtsuka E, Shimamoto T. "Unidirectional" atrioventricular conduction studied by microelectrodes. Circ Res 1960;8:600-608.

Sano T, Takayama N, Shimamoto T. Directional difference of conduction velocity in the cardiac ventricular syncytium studied by microelectrodes. Circ Res 1959;7:262-267.

Scherz P. Practical Electronics for inventors. Second edition. New York, NY: McGraw-Hill; 2007.

Shabetai R, Surawicz B, Hammill W. Monophasic Action Potentials in Man. Circulation 1968;38:341-352.

Shimizu W, Antzelevitch C. Sodium channel block with mexiletine is effective in reducing dispersion of repolarization and preventing torsade de pointes in LQT2 and LQT3 models of the long-QT syndrome. Circulation 1997;96:2038-2047.

Steenbergen C, Murphy E, Levy L, London RE. Elevation in cytosolic free calcium concentration early in myocardial ischemia in perfused rat heart. Circ Res 1987;60:700-707.

Tung L, Cysyk J. Imaging fibrillation: defibrillation in a dish. J Electrocardiol 2007;40:S62-S65.

Tung L, Zhang Y. Optical imaging of arrhythmias in tissue culture. J Electrocardiol 2006;39:S2-S6.

Valderrábano M, Lee MH, Ohara T, Lai AC, Fishbein MC, Lin SF, Karagueuzian HS, Chen PS. Dynamics of intramural and transmural reentry during ventricular fibrillation in isolated swine ventricles. Circ Res 2001;88:839-848.

Valderrábano M, Yang J, Omichi C, Kil J, Lamp ST, Qu Z, Lin SF, Karagueuzian HS, Garfinkel A, Chen PS, Weiss JN. Frequency analysis of ventricular fibrillation in swine ventricles. Circ Res 2002;90:213-222.

Weidmann, S. Effect of current flow on the membrane potential of cardiac muscle. J Physiol 1951;115:227-236.

Wu J, Biermann M, Rubart M, Zipes DP. Cytochalasin D as excitation-contraction uncoupler for optically mapping action potentials in wedges of ventricular myocardium. J Cardiovasc Electrophysiol 1998;9:1336-1347.

Wu S, Weiss JN, Chou CC, Attin M, Hayashi H, Lin SF. Dissociation of membrane potential and intracellular calcium during ventricular fibrillation. J Cardiovasc Electrophysiol 2005;16:186-192.

Wu TJ, Lin SF, Baher A, Qu Z, Garfinkel A, Weiss JN, Ting CT, Chen PS. Mother rotors and the mechanisms of D600-induced type 2 ventricular fibrillation. Circulation 2004;110:2110-2118.

Wu TJ, Lin SF, Hsieh YC, Ting CT, Chen PS. Ventricular fibrillation during no-flow global ischemia in isolated rabbit hearts. J Cardiovasc Electrophysiol 2006;17:1112-1120.

Zaitsev AV, Guha PK, Sarmast F, Kolli A, Berenfeld O, Pertsov AM, de Groot JR, Coronel R, Jalife J. Wavebreak formation during ventricular fibrillation in the isolated, regionally ischemic pig heart. Circ Res 2003;92:546-553.

Wu TJ, Lin SF, Weiss JN, Ting CT and Chen PS. Two types of ventricular fibrillation in isolated rabbit hearts: Importance of excitability and action potential duration restitution. Circulation 2002;106:1859-1866.

Zaitsev AV, Berenfeld O, Mirinov SF, Jalife J, Pertsov AM. Distribution of excitation frequencies on the epicardial and endocardial surfaces of fibrillating ventricular wall of the sheep heart. Circ Res 2000;86:408-417.

Zemlin CW, Bernus O, Matiukas A, Hyatt CJ, Pertsov AM. Extracting intramural wavefront orientation from optical upstroke shapes in whole hearts. Biophys J 2008;95:942-950.

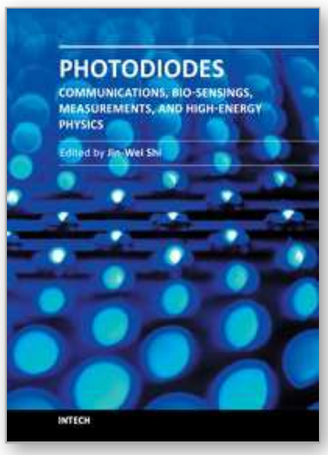

Photodiodes - Communications, Bio-Sensings, Measurements and High-Energy Physics

Edited by Associate Professor Jin-Wei Shi

ISBN 978-953-307-277-7
Hard cover, 284 pages
Publisher InTech
Published online 06, September, 2011
Published in print edition September, 2011

This book describes different kinds of photodiodes for applications in high-speed data communication, biomedical sensing, high-speed measurement, UV-light detection, and high energy physics. The photodiodes discussed are composed of several different semiconductor materials, such as InP, SiC, and Si, which cover an extremely wide optical wavelength regime ranging from infrared light to X-ray, making the suitable for diversified applications. Several interesting and unique topics were discussed including: the operation of high-speed photodiodes at low-temperature for super-conducting electronics, photodiodes for bio-medical imaging, single photon detection, photodiodes for the applications in nuclear physics, and for UV-light detection.

InTech Europe
University Campus STeP Ri
Slavka Krautzeka 83/A
51000 Rijeka, Croatia
Phone: +385 (51) 770 447
Fax: +385 (51) 686 166
www.intechopen.com

InTech China
Unit 405, Office Block, Hotel Equatorial Shanghai
No.65, Yan An Road (West), Shanghai, 200040, China
中国上海市延安西路65号上海国际贵都大饭店办公楼405单元
Phone: +86-21-62489820
Fax: +86-21-62489821

IntechOpen